Adaptive adjustable performance function based direct prescribed performance control for spacecraft flying around mission

Kun Wang[1], **Tao Meng**[1, *] **and Jiakun Lei**[1]

1. School of Aeronautics and Astronautics, Zhejiang University, Hangzhou, 310027, China

* Corresponding author's e-mail: mengtao@zju.edu.cn

Abstract. The control for spacecraft flying around mission is investigated in this paper based on the prescribed performance control. Considering the challenges in the traditional PPC framework, we design an adaptive adjustable performance function, which can self-adjust the performance requirement according to the saturation of the control input. Besides, a combined switching controller is designed and the controller behaves as a PPC in the convergence stage, and gradually switches to a nonlinear controller after entering a steady state, which can avoid the over-control problem caused by high-gain PPC after entering the steady state. Finally, the numerical simulations illustrate the effectiveness of the proposed control method.

Presenting author: Kun Wang; E-mail: wang_kun@zju.edu.cn, Affiliation: Zhejiang University; Country: People's Republic of China.
Preferred Mode of presentation: Poster.

1. Introduction

The problem of spacecraft proximity operation control has been investigated for a long time and has sufficient research results. Many nonlinear control methods have been used to achieve spacecraft proximity operation control robustly and precisely, such as sliding mode control, backstepping control, model predictive control and so on. Besides, as a method that can quantitatively characterize the transient and steady-state performance of the system, prescribed performance control (PPC) has been widely used in spacecraft relative orbit and attitude control, such as in [1] ~ [3].

However, there are some challenges in the PPC framework, which are desired further research [4]. The rationality of the prescribed performance function (PPF) is key problem in traditional PPC framework. The PPF is a user defined function that describes the performance of system, however, the actuator saturation is not considered during the design of PPF, which will lead to the performance violation because of the limited control ability. Besides, in origin PPC frame work, multiple PPFs should be designed one by one and the number of PPFs often depends on the dimensionality of the system. However, the design of multiple PPFs is not only a tedious task, but also often not intuitive for practical control systems. In practical systems, control performance is often described by absolute distance or angle. Thus, it is not necessary to design a PPF for each state.

In this paper, we proposed an adaptive adjustable performance function based direct prescribed performance controller and try to solve the problems mentioned above. The control error is summarized as the distance between the current state and the desired state and only two adaptive PPFs is designed to characterize the control accuracy for position and attitude control. The adaptive PPF is a self-adjust function according to the saturation of the control input. Besides, another robust nonlinear controller is designed and the switch of the nonlinear controller and distance based PPC is achieved by using a smooth step function. Stability analysis shows the feasibility of switching between the two controllers. Finally, numerical simulation illustrates the effectiveness of the proposed controller.

2. Preliminaries and Problem Statement

In this section, we give spacecraft relative position dynamics and attitude dynamics first, then the problem investigated in this paper is formulated. The coordinate system used in this paper is given as follows: the Earth-centred inertial (ECI) frame $\mathcal{I}$, the body frame of the chaser spacecraft $\mathcal{B}$ and the vehicle-velocity-local-horizontal (VVLH) frame $\mathcal{L}$. The origin of frame $\mathcal{L}$ locates at the centre of the target spacecraft. The following notations are used in this paper: $\|\cdot\|$ to represent the norm of a vector, $\mathrm{Tanh}(\mathbf{x}) \triangleq [\tanh(x_1), \tanh(x_2), \tanh(x_3)]^T$, $\mathbf{a}^\times$ is the skew symmetric matrix form of vector $\mathbf{a}$, $\mathbf{0}_{n\times n}$ denotes the $n\times n$ zero matrix, $\mathbf{I}_{n\times n}$ denotes the $n\times n$ identity matrix, $\lambda_{\min}(\cdot)$ denotes the minimum eigenvalue of a matrix.

Lemma 1 For any $\mu > 0$ and $x \in \mathbb{R}$, the following formula will be satisfied:

$$0 \leqslant |x| - x\tanh\left(\frac{x}{\mu}\right) \leqslant 0.2785\mu$$

2.1. Relative Position Dynamics

The relative position dynamics between the chaser spacecraft and the target spacecraft can be written as:

$$\begin{aligned} \dot{\mathbf{r}} &= \mathbf{v} \\ m\dot{\mathbf{v}} &= -\mathbf{C}\mathbf{v} - \mathbf{D}\mathbf{r} + \mathbf{g} + \mathbf{F} - \mathbf{d}_f \end{aligned} \tag{1}$$

where $\mathbf{r}$ and $\mathbf{v}$ denote the relative position and velocity vector between the chaser and the target, $\mathbf{F}$ is the orbit control force expressed in frame $\mathcal{L}$, m is the mass of the chaser spacecraft, $\mathbf{d}_f$ denotes the external disturbance force and unmodeled dynamics. Besides, the detailed expressions of matrices $\mathbf{C}$ and $\mathbf{D}$ can be found in [5]. We denote $\mathbf{r}_d$ as the desired flying around trajectory, which is second order continuous differentiable, i.e. $\dot{\mathbf{r}}_d$, $\ddot{\mathbf{r}}_d$ exist. Then the position error can be expressed as $\mathbf{r}_e = \mathbf{r} - \mathbf{r}_d$.

2.2. Attitude Dynamics

We suppose that the relative navigation devices are installed on the $+X$ side of the chaser spacecraft, i.e. the current point direction vector of the navigation device expressed in frame $\mathcal{B}$ is $\mathbf{x}^{\mathcal{B}} = [1,0,0]^T$. The unit direction vector of the target spacecraft expressed in frame $\mathcal{B}$ is denoted as $\mathbf{x}_d^{\mathcal{B}}$, then the attitude error quaternion $\mathbf{q}_e$ can be expressed as [6]:

$$\mathbf{q}_e = \begin{bmatrix} \mathbf{q}_{ev} \\ q_{e4} \end{bmatrix} = \begin{bmatrix} \dfrac{(\mathbf{x}_d^{\mathcal{B}})^\times \mathbf{x}^{\mathcal{B}}}{\sqrt{2(1+(\mathbf{x}^{\mathcal{B}})^T \mathbf{x}_d^{\mathcal{B}})}} \\ \sqrt{\dfrac{1+(\mathbf{x}^{\mathcal{B}})^T \mathbf{x}_d^{\mathcal{B}}}{2}} \end{bmatrix} \tag{2}$$

then the attitude error kinematics can be written as [5]

$$\begin{aligned} \dot{\mathbf{q}}_{ev} &= \mathbf{Q}\boldsymbol{\omega}_e \\ \mathbf{Q} &= \frac{1}{2}(\mathbf{q}_{ev}^\times + q_{e4}\mathbf{I}_3) \end{aligned} \tag{3}$$

and the attitude dynamics can be written as

$$\mathbf{J}\dot{\boldsymbol{\omega}} = -\boldsymbol{\omega}^\times \mathbf{J}\boldsymbol{\omega} + \mathbf{T} + \mathbf{d}_t \tag{4}$$

where $\boldsymbol{\omega}$ denotes the angular velocity of the chaser, $\mathbf{J}$ is the inertia matrix of the chaser, $\mathbf{T}$ denotes the control torque and $\mathbf{d}_t$ denotes the external disturbance torque and unmodeled dynamics. Let $\boldsymbol{\omega}_d$ denote the desired angular velocity and then $\boldsymbol{\omega}_e = \boldsymbol{\omega} - \mathbf{E}\boldsymbol{\omega}_d$, where the corresponding rotation matrix $\mathbf{E}$ can be given as $\mathbf{E} = (q_{e4}^2 - \mathbf{q}_{ev}^T\mathbf{q}_{ev})\mathbf{I}_3 + 2\mathbf{q}_{ev}\mathbf{q}_{ev}^T - 2q_{e4}\mathbf{q}_{ev}^\times$.

2.3. Spacecraft 6-DOF dynamics model

We define the transformed errors as $\varepsilon_r = \dfrac{\mathbf{r}_e^T\mathbf{r}_e}{\sigma_r}$ and $\varepsilon_q = \dfrac{\mathbf{q}_{ev}^T\mathbf{q}_{ev}}{\sigma_q}$. The transformed error vector can be defined as $\boldsymbol{\varepsilon} = \left[\varepsilon_r, \varepsilon_q\right]^T$, then the dynamics of $\boldsymbol{\varepsilon}$ can be written as

$$\dot{\boldsymbol{\varepsilon}} = -\mathbf{A}\boldsymbol{\varepsilon} + \mathbf{B}\mathbf{z}_1 \tag{5}$$

where $\mathbf{A} = \begin{bmatrix} \dfrac{\dot{\sigma}_r}{\sigma_r} & 0 \\ 0 & \dfrac{\dot{\sigma}_q}{\sigma_q} \end{bmatrix}$, $\mathbf{B} = \begin{bmatrix} \dfrac{2\mathbf{r}_e^T}{\sigma_r} & \mathbf{0}_{1\times3} \\ \mathbf{0}_{1\times3} & \dfrac{2\mathbf{q}_{ev}^T\mathbf{Q}}{\sigma_q} \end{bmatrix}$, $\mathbf{z}_1 = \left[\mathbf{v}_e^T, \boldsymbol{\omega}_e^T\right]^T$. We define $\mathbf{x} = \left[\mathbf{v}^T, \boldsymbol{\omega}^T\right]^T$, $\mathbf{x}_d = \left[\mathbf{v}_d^T, \boldsymbol{\omega}_d^T\right]^T$ and $\mathbf{z}_2 = \mathbf{x} - \mathbf{x}_v$, where $\mathbf{x}_v$ is the virtual control to be designed. Then the spacecraft 6-DOF dynamics model can be written as

$$\begin{aligned} \dot{\boldsymbol{\varepsilon}} &= -\mathbf{A}\boldsymbol{\varepsilon} + \mathbf{B}\mathbf{z}_1 \\ \mathbf{M}\dot{\mathbf{z}}_2 &= f(\mathbf{x}) + \mathbf{u} + \mathbf{d} \end{aligned} \tag{6}$$

where $\mathbf{M} = \begin{bmatrix} m\mathbf{I}_{3\times3} & \mathbf{0}_{3\times3} \\ \mathbf{0}_{3\times3} & \mathbf{J} \end{bmatrix}$, $\mathbf{u} = \begin{bmatrix} \mathbf{F} \\ \mathbf{T} \end{bmatrix}$, $f(\mathbf{x}) = \begin{bmatrix} -\mathbf{C}\mathbf{v} - \mathbf{D}\mathbf{r} + \mathbf{g} \\ -\boldsymbol{\omega}^\times\mathbf{J}\boldsymbol{\omega} \end{bmatrix}$ and $\mathbf{d} = \begin{bmatrix} \mathbf{d}_f \\ \mathbf{d}_t \end{bmatrix} - \dot{\mathbf{x}}_v$.

2.4. Problem Formulation

Assumption 1: The uncertainty term $\mathbf{d}$ is a bounded term, i.e. $\|\mathbf{d}\| \leqslant d_m$.

The control objective of this paper is to design a controller that can guarantee the position and attitude control error to satisfy $\|\mathbf{r}_e\| \leqslant \sqrt{\sigma_r(t)}$ and $\|\mathbf{q}_{ev}\| \leqslant \sqrt{\sigma_q(t)}$ under input saturation, where $\sigma_r(t)$ and $\sigma_q(t)$ are continuous functions.

3. Main Results

3.1. Adaptive Adjustable Performance Function Design

The control force and torque generated by controllers are denoted as $\mathbf{F}_c$ and $\mathbf{T}_c$, and $\mathbf{F} = \mathrm{Sat}(\mathbf{F}_c)$, $\mathbf{T} = \mathrm{Sat}(\mathbf{T}_c)$ are the practically applied force and torque, where $\mathrm{Sat}(\cdot)$ is the saturation function. The adaptive adjustable performance functions are designed as

$$\begin{aligned} \sigma_r(t) &= \sigma_{r0}e^{-b_r t} + \sigma_{r\infty} + \Delta\sigma_r \\ \sigma_q(t) &= \sigma_{q0}e^{-b_q t} + \sigma_{q\infty} + \Delta\sigma_q \end{aligned} \tag{7}$$

where σ_{r0}, σ_{q0} are the initial values related to the initial position and attitude control error and satisfy $\|\mathbf{r}_e(0)\| < \sigma_{r0}$, $\|\mathbf{q}_{ev}(0)\| < \sigma_{q0}$, b_r, b_q are the tuneable constants and $\sigma_{r\infty}$, $\sigma_{q\infty}$ represent the steady performance requirements. Besides, $\Delta\sigma_r$ and $\Delta\sigma_q$ are the modification signals to origin performance function and generated by the following system:

$$\begin{aligned} \Delta\dot{\sigma}_r &= -k_r\Delta\sigma_r + \Delta\nu, \Delta\sigma_r(0) = 0 \\ \Delta\dot{\nu} &= -k_\nu\Delta\nu + p_r\left\|\mathrm{Tanh}(\Delta\mathbf{F})\right\|, \Delta\nu(0) = 0 \end{aligned} \tag{8}$$

$$\begin{aligned} \Delta\dot{\sigma}_q &= -k_q\Delta\sigma_q + \Delta w, \Delta\sigma_q(0) = 0 \\ \Delta\dot{w} &= -k_w\Delta w + p_q\left\|\mathrm{Tanh}(\Delta\mathbf{T})\right\|, \Delta\nu(0) = 0 \end{aligned} \tag{9}$$

where $k_r > 0$, $k_\nu > 0$, $k_q > 0$, $k_w > 0$, $\Delta\mathbf{F} = \mathbf{F} - \mathbf{F}_c$, $\Delta\mathbf{T} = \mathbf{T} - \mathbf{T}_c$ and p_r, p_q are tuneable positive constants.

3.2. Direct Prescribed Performance Controller Design

The definition of the transformed errors means that $\varepsilon_r < 1$ and $\varepsilon_q < 1$ when the performance constraints are satisfied.

Then the controller can be designed as

$$\mathbf{u} = -f(\mathbf{x}) - k_2\mathbf{z}_2 - d_m \operatorname{Tanh}(\frac{\mathbf{z}_2}{\mu}) + \mathbf{\Phi}\mathbf{u}_{ppc} + (\mathbf{I}_{6\times6} - \mathbf{\Phi})\mathbf{u}_{nc} \tag{10}$$

The virtual control is designed as

$$\mathbf{x}_v = -k_1\begin{bmatrix}\mathbf{r}_e \\ \mathbf{Q}^T\mathbf{q}_{ev}\end{bmatrix} + \mathbf{x}_d \tag{11}$$

and the PPC term and nonlinear controller term are designed as

$$\begin{aligned}\mathbf{u}_{ppc} &= -\mathbf{H}^T \\ \mathbf{u}_{nc} &= -\mathbf{K}_3\begin{bmatrix}\mathbf{r}_e \\ \mathbf{Q}^T\mathbf{q}_{ev}\end{bmatrix}\end{aligned} \tag{12}$$

where $\mathbf{H} = \begin{bmatrix}\frac{2\varepsilon_r}{1-\varepsilon_r^2}\frac{\mathbf{r}_e^T}{\sigma_r} & \frac{2\varepsilon_q}{1-\varepsilon_q^2}\frac{\mathbf{q}_{ev}^T\mathbf{Q}}{\sigma_q}\end{bmatrix}$, $\mathbf{K}_3 = \begin{bmatrix}k_{3r}\mathbf{I}_{3\times3} & \\ & k_{3q}\mathbf{I}_{3\times3}\end{bmatrix}$. The diagonal matrix $\mathbf{\Phi}$ is defined as

$$\mathbf{\Phi} = \begin{bmatrix}\Phi_r\mathbf{I}_{3\times3} & \\ & \Phi_q\mathbf{I}_{3\times3}\end{bmatrix} \tag{13}$$

where Φ_r and Φ_q are two variables that related to the position and attitude control performance and can be defined as

$$\Phi_i(\varepsilon_i) = \begin{cases}1 & \text{if} \quad \varepsilon_i > \delta_{i2} \text{or} \sigma_i > 1 \\ \frac{1}{2}\left[\tanh\left(\frac{\kappa(2\varepsilon_i - \delta_{i1} - \delta_{i2})}{2\sqrt{(\delta_{i2} - \varepsilon_i)(\varepsilon_i - \delta_{i1})}}\right) + 1\right] & \text{if} \quad \delta_{i1} \leqslant \varepsilon_i \leqslant \delta_{i2} \\ 0 & \text{if} \quad \varepsilon_i < \delta_{i1}\end{cases} \tag{14}$$

where $i = r, q$, δ_{i1} , δ_{i2} are user defined parameters. From Eq.(14), we can indicate that the variables $\Phi_i(i = r, q) \in [0,1]$ and the control input will be switched between the PPC controller and the nonlinear controller.

Then we can give the following theorem:

Theorem 1: Considering the spacecraft 6-DOF dynamics model Eq.(6), the controller is designed as Eq.(10) and the performance functions are designed as Eq.(7), then the transformed error will be maintained in the interval $(0,1)$ and the control objective can be achieved.

Proof:

The candidate Lyapunov function can be designed as

$$V_1 = \frac{1}{2}\log\left(\frac{1}{1-\varepsilon_r^2}\frac{1}{1-\varepsilon_q^2}\right) \tag{15}$$

Taking the time derivative of V_1 yields

$$\begin{aligned}\dot{V}_1 &= \begin{bmatrix}\frac{\varepsilon_r}{1-\varepsilon_r^2} & \frac{\varepsilon_q}{1-\varepsilon_q^2}\end{bmatrix}\dot{\boldsymbol{\varepsilon}} = \begin{bmatrix}\frac{\varepsilon_r}{1-\varepsilon_r^2} & \frac{\varepsilon_q}{1-\varepsilon_q^2}\end{bmatrix}(-\mathbf{A}\boldsymbol{\varepsilon} + \mathbf{B}\mathbf{z}_1) \\ &= -\frac{\dot{\sigma}_r}{\sigma_r}\frac{\varepsilon_r^2}{1-\varepsilon_r^2} - \frac{\dot{\sigma}_q}{\sigma_q}\frac{\varepsilon_q^2}{1-\varepsilon_q^2} + \mathbf{H}\left(\mathbf{x}_v + \mathbf{z}_2 - \mathbf{x}_d\right)\end{aligned} \tag{16}$$

Considering the following inequality

$$\mathbf{q}_{ev}^T\mathbf{Q}\mathbf{Q}^T\mathbf{q}_{ev} \leqslant \lambda_{\min}\left(\mathbf{Q}\mathbf{Q}^T\right)\|\mathbf{q}_{ev}\|^2 \leqslant \frac{q_{e4}^2}{4}\|\mathbf{q}_{ev}\|^2 \tag{17}$$

and substituting Eq.(11) into Eq.(16) yields

$$\dot{V}_1 = -(2k_1 + \frac{\dot{\sigma}_r}{\sigma_r})\frac{\varepsilon_r^2}{1-\varepsilon_r^2} - \frac{2k_1\varepsilon_q}{1-\varepsilon_q^2}\frac{\mathbf{q}_{ev}^T\mathbf{Q}\mathbf{Q}^T\mathbf{q}_{ev}}{\sigma_q} - \frac{\dot{\sigma}_q}{\sigma_q}\frac{\varepsilon_q^2}{1-\varepsilon_q^2} + \mathbf{H}\mathbf{z}_2$$
$$\leqslant -(2k_1 + \frac{\dot{\sigma}_r}{\sigma_r})\frac{\varepsilon_r^2}{1-\varepsilon_r^2} - \left(\frac{q_{e4}^2}{2}k_1 + \frac{\dot{\sigma}_q}{\sigma_q}\right)\frac{\varepsilon_q^2}{1-\varepsilon_q^2} + \mathbf{H}\mathbf{z}_2 \tag{18}$$

Then define the following Lyapunov function

$$V = V_1 + \frac{1}{2}\mathbf{z}_2^T\mathbf{M}\mathbf{z}_2 \tag{19}$$

Taking the time derivative of V and substituting Eq.(6) yields

$$\dot{V} \leqslant -(2k_1 + \frac{\dot{\sigma}_r}{\sigma_r})\frac{\varepsilon_r^2}{1-\varepsilon_r^2} - \left(\frac{q_{e4}^2}{2}k_1 + \frac{\dot{\sigma}_q}{\sigma_q}\right)\frac{\varepsilon_q^2}{1-\varepsilon_q^2} + \mathbf{H}\mathbf{z}_2 + \mathbf{z}_2^T\left(f(\mathbf{x}) + \mathbf{u} + \mathbf{d}\right) \tag{20}$$

Then substituting Eq.(10) into Eq.(20) yields

$$\dot{V} \leqslant -(2k_1 + \frac{\dot{\sigma}_r}{\sigma_r})\frac{\varepsilon_r^2}{1-\varepsilon_r^2} - \left(\frac{q_{e4}^2}{2}k_1 + \frac{\dot{\sigma}_q}{\sigma_q}\right)\frac{\varepsilon_q^2}{1-\varepsilon_q^2} + \mathbf{H}\mathbf{z}_2 + \mathbf{z}_2^T\left(-k_2\mathbf{z}_2 - d_m\,\mathrm{Tanh}(\frac{\mathbf{z}_2}{\mu}) + \mathbf{\Phi}\mathbf{u}_{ppc} + (\mathbf{I}_{6\times6} - \mathbf{\Phi})\mathbf{u}_{nc} + \mathbf{d}\right)$$
$$= -(2k_1 + \frac{\dot{\sigma}_r}{\sigma_r})\frac{\varepsilon_r^2}{1-\varepsilon_r^2} - \left(\frac{q_{e4}^2}{2}k_1 + \frac{\dot{\sigma}_q}{\sigma_q}\right)\frac{\varepsilon_q^2}{1-\varepsilon_q^2} - k_2\mathbf{z}_2^T\mathbf{z}_2 + \mathbf{H}(\mathbf{I}_{6\times6} - \mathbf{\Phi})\mathbf{z}_2 - \mathbf{K}_3\left[\mathbf{r}_e^T \quad \mathbf{q}_{ev}^T\mathbf{Q}\right](\mathbf{I}_{6\times6} - \mathbf{\Phi})\mathbf{z}_2$$
$$-d_m\mathbf{z}_2^T\,\mathrm{Tanh}(\frac{\mathbf{z}_2}{\mu}) + \mathbf{z}_2^T\mathbf{d}$$
$$= -(2k_1 + \frac{\dot{\sigma}_r}{\sigma_r})\frac{\varepsilon_r^2}{1-\varepsilon_r^2} - \left(\frac{q_{e4}^2}{2}k_1 + \frac{\dot{\sigma}_q}{\sigma_q}\right)\frac{\varepsilon_q^2}{1-\varepsilon_q^2} - k_2\mathbf{z}_2^T\mathbf{z}_2 + (1-\Phi_r)\left(\frac{\varepsilon_r}{1-\varepsilon_r^2}\frac{1}{\sigma_r} - k_{3r}\right)\mathbf{r}_e^T\mathbf{z}_{2r} \tag{21}$$
$$+(1-\Phi_q)\left(\frac{\varepsilon_q}{1-\varepsilon_q^2}\frac{1}{\sigma_q} - k_{3q}\right)\mathbf{q}_{ev}^T\mathbf{Q}\mathbf{z}_{2q} - d_m\mathbf{z}_2^T\,\mathrm{Tanh}(\frac{\mathbf{z}_2}{\mu}) + \mathbf{z}_2^T\mathbf{d}$$
$$\leqslant -(2k_1 + \frac{\dot{\sigma}_r}{\sigma_r})\frac{\varepsilon_r^2}{1-\varepsilon_r^2} - \left(\frac{q_{e4}^2}{2}k_1 + \frac{\dot{\sigma}_q}{\sigma_q}\right)\frac{\varepsilon_q^2}{1-\varepsilon_q^2} - k_2\mathbf{z}_2^T\mathbf{z}_2 + (1-\Phi_r)\left(\frac{\varepsilon_r}{1-\varepsilon_r^2}\frac{1}{\sigma_r} - k_{3r}\right)\mathbf{r}_e^T\mathbf{z}_{2r}$$
$$+(1-\Phi_q)\left(\frac{\varepsilon_q}{1-\varepsilon_q^2}\frac{1}{\sigma_q} - k_{3q}\right)\mathbf{q}_{ev}^T\mathbf{Q}\mathbf{z}_{2q} + d_m\sum_{i=1}^{6}\left(|z_{2i}| - z_{2i}\tanh(\frac{z_{2i}}{\mu})\right)$$

Here we discuss the following two cases:

1) case 1: when $\varepsilon_r > \delta_{r2}$ and $\varepsilon_q > \delta_{q2}$, $1-\Phi_r = 1-\Phi_q = 0$, then Eq.(21) can be deduced as

$$\dot{V} \leqslant -(2k_1 + \frac{\dot{\sigma}_r}{\sigma_r})\frac{\varepsilon_r^2}{1-\varepsilon_r^2} - \left(\frac{q_{e4}^2}{2}k_1 + \frac{\dot{\sigma}_q}{\sigma_q}\right)\frac{\varepsilon_q^2}{1-\varepsilon_q^2} - k_2\mathbf{z}_2^T\mathbf{z}_2 + 1.671 d_m\mu \tag{22}$$

selecting proper k_1 to make sure that $2k_1 + \frac{\dot{\sigma}_r}{\sigma_r} > 0$ and $\frac{q_{e4}^2}{2}k_1 + \frac{\dot{\sigma}_q}{\sigma_q} > 0$, then we can have

$$\dot{V} \leqslant -b_0 V + e_0 \tag{23}$$

where $b_0 = \min(2k_1 + \frac{\dot{\sigma}_r}{\sigma_r}, \frac{q_{e4}^2}{2}k_1 + \frac{\dot{\sigma}_q}{\sigma_q}, 2k_2)$, $e_0 = 1.671 d_m\mu$.

2) case 2: when $\varepsilon_r \leqslant \delta_{r2}$ and $\varepsilon_q \leqslant \delta_{q2}$, then Eq.(21) can be deduced as

$$\dot{V} \leqslant -(2k_1 + \frac{\dot{\sigma}_r}{\sigma_r})\frac{\varepsilon_r^2}{1-\varepsilon_r^2} - \left(\frac{q_{e4}^2}{2}k_1 + \frac{\dot{\sigma}_q}{\sigma_q}\right)\frac{\varepsilon_q^2}{1-\varepsilon_q^2} - k_2\mathbf{z}_2^T\mathbf{z}_2$$
$$+\left|\frac{1}{\sigma_r}\frac{\varepsilon_r}{1-\varepsilon_r^2} - k_{3r}\right|\|\mathbf{r}_e\|\|\mathbf{z}_{2r}\| + \left|\frac{1}{\sigma_q}\frac{\varepsilon_q}{1-\varepsilon_q^2} - k_{3q}\right|\|\mathbf{q}_{ev}\|\|\mathbf{z}_{2q}\|\|\mathbf{Q}\| + 1.671 d_m\mu \tag{24}$$

Considering that function $g(x)=\dfrac{x}{1-x^2}(x\geqslant 0)$ is a positive monotonically increasing function, then we have $g(\varepsilon_r)<g(\delta_{r2})\triangleq d_r$ and $g(\varepsilon_q)<g(\delta_{q2})\triangleq d_q$. Selecting proper k_{3r} and k_{3q} to make sure that $\left|\dfrac{1}{\sigma_r}\dfrac{\varepsilon_r}{1-\varepsilon_r^2}-k_{3r}\right|<c_r$ and $\left|\dfrac{1}{\sigma_q}\dfrac{\varepsilon_q}{1-\varepsilon_q^2}-k_{3q}\right|<c_q$, considering that $\|\mathbf{Q}\|<1$, we have

$$\begin{aligned}\dot{V}&\leqslant-(2k_1+\frac{\dot{\sigma}_r}{\sigma_r})\frac{\varepsilon_r^2}{1-\varepsilon_r^2}-\left(\frac{q_{e4}^2}{2}k_1+\frac{\dot{\sigma}_q}{\sigma_q}\right)\frac{\varepsilon_q^2}{1-\varepsilon_q^2}-k_2\mathbf{z}_2^T\mathbf{z}_2+\frac{c_r}{2}\|\mathbf{r}_e\|^2+\frac{c_q}{2}\|\mathbf{q}_{ev}\|^2+\frac{\max(c_r,c_q)}{2}\|\mathbf{z}_2\|^2+1.671d_m\mu\\&\leqslant-(2k_1+\frac{\dot{\sigma}_r}{\sigma_r})\frac{\varepsilon_r^2}{1-\varepsilon_r^2}-\left(\frac{q_{e4}^2}{2}k_1+\frac{\dot{\sigma}_q}{\sigma_q}\right)\frac{\varepsilon_q^2}{1-\varepsilon_q^2}-\left(k_2-\frac{\max(c_r,c_q)}{2}\right)\mathbf{z}_2^T\mathbf{z}_2+\frac{c_r\delta_{r2}}{2}+\frac{c_q\delta_{q2}}{2}+1.671d_m\mu\end{aligned}\tag{25}$$

Let $k_2>\dfrac{\max(c_r,c_q)}{2}$, then we have

$$\dot{V}\leqslant-b_1V+e_1\tag{26}$$

where $b_1=\min\left(2k_1+\dfrac{\dot{\sigma}_r}{\sigma_r},\dfrac{q_{e4}^2}{2}k_1+\dfrac{\dot{\sigma}_q}{\sigma_q},k_2-\dfrac{\max(c_r,c_q)}{2}\right)$, $e_1=\dfrac{c_r\delta_{r2}}{2}+\dfrac{c_q\delta_{q2}}{2}+1.671d_m\mu$.

The results of other cases are same as the above two cases. Then it can be deduced that the following inequality always holds in different cases

$$\dot{V}\leqslant-\gamma V+\rho\tag{27}$$

where $\gamma>0$ and $\rho>0$. Then it can be concluded that the transformed error will be maintained in the desired interval and the control objective can be achieved.

4. Numerical Simulations

In this section, we conduct the numerical simulations to illustrate the effectiveness of the proposed control method. The simulations are conducted as nominal part and practical part and the control frequency is set as 1s.

4.1. Simulation Settings

The mass of the chaser spacecraft is 20kg, and the initial orbit elements of the target spacecraft are listed in Table 1, the inertia of the chaser is $\mathbf{J}=\begin{bmatrix}0.6604 & 0.0145 & 0.0081\\0.0145 & 0.8474 & 0.0354\\0.0081 & 0.0354 & 0.7839\end{bmatrix}$.

Table 1. Initial Orbit Elements of the Target Spacecraft

Parameters	Value	Unit
Semimajor axis	42139	km
Eccentricity	0.002	-
Inclination	5.3707	deg
RAAN	51.2091	deg
Argument of perigee	236.3791	deg
Mean anomaly	59.4097	deg

The desired trajectory is generated as the trajectory in [5], where the radius of trajectory is set as 60m, the inclination of the trajectory is set as 45deg and the period of flying around is set as 3600s. The initial position of the chaser is set as $\mathbf{r}(0)=\begin{bmatrix}61 & -1 & 0\end{bmatrix}^T$ m, the initial velocity is set as $\mathbf{v}(0)=\begin{bmatrix}0.01 & -0.01 & 0.02\end{bmatrix}^T$ m/s, the initial attitude is set as $\mathbf{q}(0)=\begin{bmatrix}0.6771 & -0.6225 & -0.2627 & 0.2916\end{bmatrix}^T$, and the initial angular velocity is set as $\boldsymbol{\omega}(0)=\begin{bmatrix}0.8 & -0.6 & 0.9\end{bmatrix}^T$ °/s.

Besides, the control parameters are selected as: $\sigma_{r0}=10$, $\sigma_{q0}=0.1$, $\sigma_{r\infty}=0.03$, $\sigma_{q\infty}=0.001$, $b_r=b_q=0.01$, $k_1=0.05$, $k_2=0.55$, $k_{3r}=0.1$, $k_{3q}=0.3$, $d_m=0.001$, $\delta_{r1}=\delta_{q1}=0.4$, $\delta_{r2}=\delta_{q2}=0.6$, $\mu=0.1$,

$k_r = k_q = 0.1$, $k_v = k_w = 0.2$, $p_r = 0.05$, $p_q = 0.01$. The maximum control force is set as 0.1N and the maximum control torque is set as 0.01Nm.

4.2. Nominal Simulation

Here we give the results of nominal simulation, from **Figure 1**~ **Figure 4**.

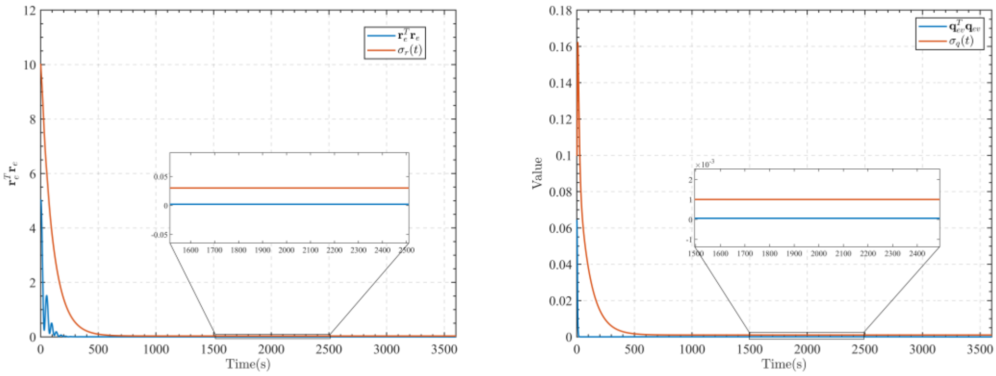

Figure 1. Time Response of Position and Attitude Control Error

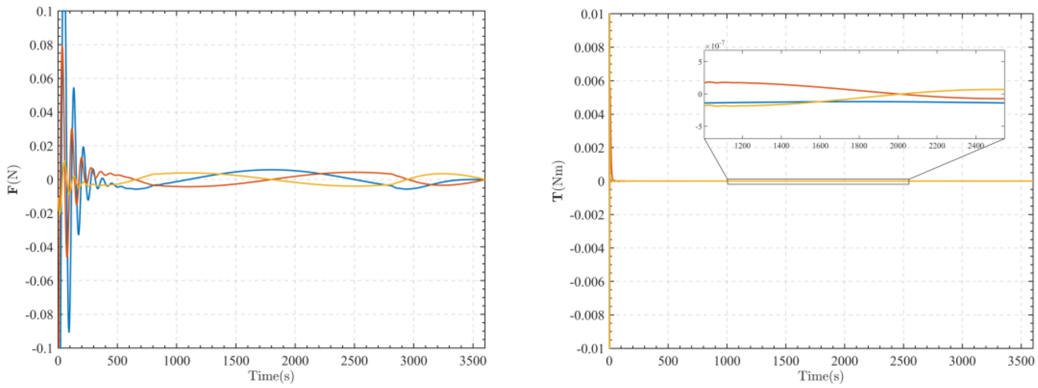

Figure 2. Time Response of Control Force and Torque

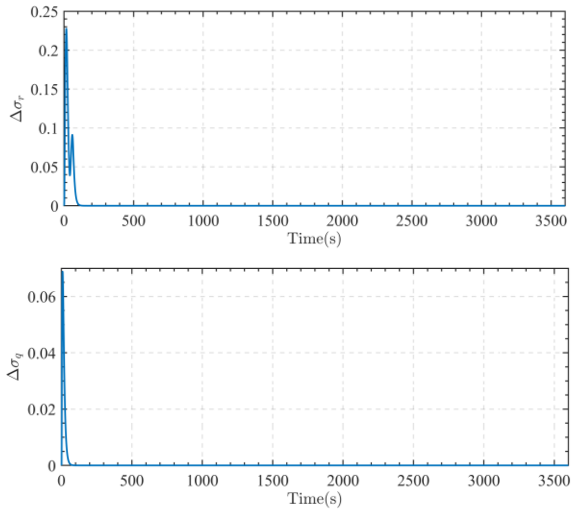

Figure 3. Time Response of the Modification Signal of Performance Function

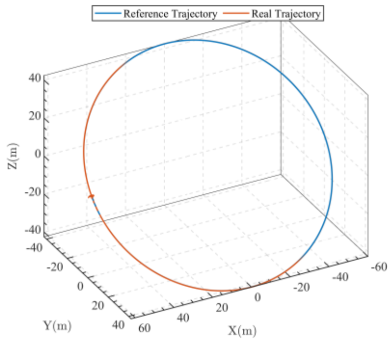

Figure 4. 3D Trajectory of the Flying Around Mission

Figure 1 shows the control error curves and we can conclude that the control objective is totally achieved. It can be observed that the control force and torque are saturated and the performance functions are modified at the same time from **Figure 2** and **Figure 3**. Thus, the designed adaptive performance functions are effective.

4.3. Practical Simulation

In practical simulation, the external disturbances are added to the chaser and set as

$$\mathbf{d}_f = \begin{cases} 0.1\left[\sin(0.02t) \quad \cos(0.01t) \quad \sin(0.02t+0.5)\right]^T N & \text{if} \quad t \in [1500,1510] \\ 0.005\left[\sin(0.02t) \quad \cos(0.01t) \quad \sin(0.02t+0.5)\right]^T N & \text{else} \end{cases}$$

$$\mathbf{d}_t = \begin{cases} 0.01\left[\sin(0.03t) \quad \cos(0.02t) \quad \sin(0.01t+0.5)\right]^T Nm & \text{if} \quad t \in [2000,2010] \\ 0.001\left[\sin(0.03t) \quad \cos(0.02t) \quad \sin(0.01t+0.5)\right]^T Nm & \text{else} \end{cases}$$

The simulation results are shown from Figure 5 ~ Figure 6.

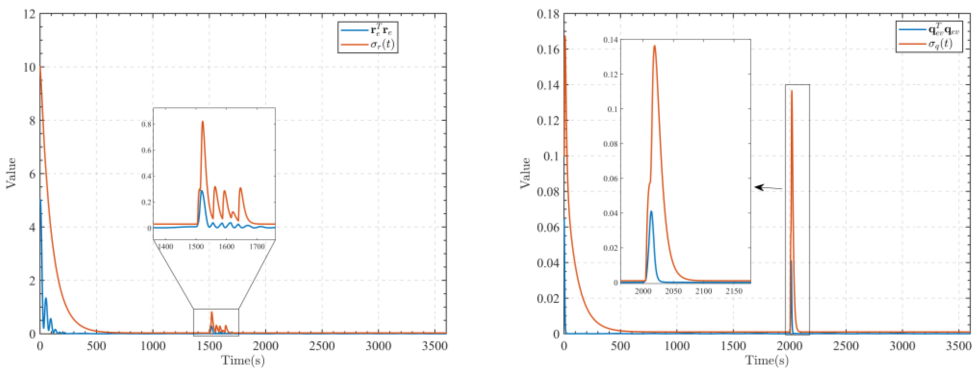

Figure 5. Time Response of Position and Attitude Control Error under External Disturbance

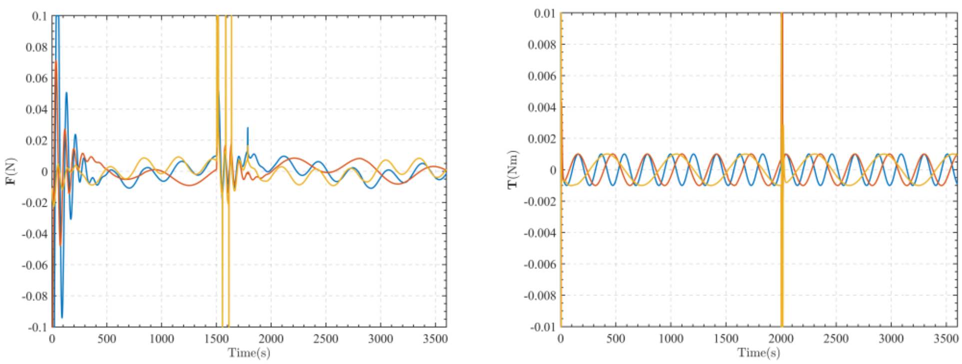

Figure 6. Time Response of Control Force and Torque under External Disturbance

In the practical simulation, we add some large external disturbance force and torque, which are equal to the maximum control output. From **Figure 5**, it can be observed that the performance function will adjust the performance requirements and then converge to the required performance when the saturation is eliminated. From **Figure 6**, we can observe that the controller can switch to the PPC mode when the large disturbances are added and then switch to the nonlinear control mode when the disturbances being small. These phenomena illustrate the effectiveness of the proposed method.

5. Conclusions

In this paper, the spacecraft flying around control is investigated. An adaptive adjustable performance function based direct prescribed performance controller is proposed, which can deal with the control input saturation and don't need complicated performance function. The nominal simulation illustrates the effectiveness of the proposed controller and the practical simulation illustrates the effectiveness of the adaptive adjustable performance functions.

Reference

[1] Li, Q., Gao, D., Sun, C., Song, S., Niu, Z. and Yang, Y. 2023 Prescribed performance-based robust inverse optimal control for spacecraft proximity operations with safety concern. Aerosp. Sci. Technol. **136** 108229.

[2] Wu, X., Luo, S., Yang, S. and Wei, C. 2022 Adaptive appointed-time formation tracking control for multiple spacecraft with collision avoidance under a dynamic event-triggered mechanism. Adv. Space Res. **70(11)** 3552-3567.

[3] Zhang, Y. C., Wu, G. Q., Yuan, J., Yang, X. Y. and Song, S. M. 2023 Composite neural learning based appointed-time safe approach control under full-state constraints. Adv. Space Res (Preprint).

[4] Bu, X. 2023 Prescribed performance control approaches, applications and challenges: A comprehensive survey. Asian J. Control **25(1)** 241-261.

[5] Wang, K., Meng, T., Wang, W., Song, R. and Jin, Z. 2022 Finite-time extended state observer based prescribed performance fault tolerance control for spacecraft proximity operations. Adv. Space Res. **70(5)** 1270-1284.

[6] Roberts, A. and Tayebi, A. 2010 Adaptive position tracking of VTOL UAVs. IEEE Trans. Rob. **27(1)** 129-142.

Authors' background

Your Name	Title*	Research Field	Personal website
Kun Wang	Ph.D. Candidate	Spacecraft attitude and orbit control	https://scholar.google.com/citations?user=DEd9ppYAAAAJ&hl=zh-CN
Tao Meng	Full Professor	Spacecraft attitude and orbit control；Spacecraft formation control	https://person.zju.edu.cn/meng
Jiakun Lei	Ph.D. Candidate	Spacecraft attitude control	